Electronic Supplementary Information (ESI)

Boronate- and borinate-based π-systems for blue thermally activated delayed fluorescence materials

Kyohei Matsuo[a] and Takuma Yasuda*[ab]

[a] INAMORI Frontier Research Center (IFRC), Kyushu University,
744 Motooka, Nishi-ku, Fukuoka 819-0395, Japan

[b] Department of Applied Chemistry, Graduate School of Engineering,
Kyushu University, 744 Motooka, Nishi-ku, Fukuoka 819-0395, Japan

[*] E-mail: yasuda@ifrc.kyushu-u.ac.jp

Table of Contents:

1. Materials, Synthesis, and Characterization S2
2. X-ray Crystallographic Analysis S12
3. Photophysical Properties S14
4. Computational Method S20
5. OLED Fabrication and Characterization S24
6. References S25

1. Materials, Synthesis, and Characterization

All reagents and anhydrous solvents were purchased from Sigma-Aldrich, Tokyo Chemical Industry (TCI), or FUJIFILM Wako Pure Chemical Corporation, and were used without further purification unless otherwise indicated. (2-bromophenyl)(*tert*-butyl)sulfane,[1] 2-methoxyphenylboronic acid,[2] 2,7-dimethyl-10*H*-spiro[acridine-9,9'-fluorene] (**5**),[3] 2,8-bis(diphenylphosphine oxide)dibenzo[b,d]furan (PPF),[4] and 9-phenyl-3,9'-bicarbazole (CCP)[5] were prepared according to the literature procedure. 2,3,6,7,10,11-Hexacyano-1,4,5,8,9,12-hexaazatriphenylene (HAT-CN) was donated by the Nippon Soda Co., Ltd. and purified by vacuum sublimation before use. Other OLED materials were purchased from E-Ray Optoelectronic Technology Co., Ltd. and were used without further purification. All reactions were performed under a N_2 atmosphere. Final products **1–3** were purified by temperature-gradient vacuum sublimation to provide highly pure materials for photophysical property measurements and OLED device fabrications. ^{1}H and ^{13}C NMR spectra were recorded on a Bruker Avance III 400 spectrometer (400 MHz, for ^{1}H and 100 MHz for ^{13}C, respectively). Chemical shifts of ^{1}H and ^{13}C NMR signals were quoted to tetramethylsilane (δ = 0.00 ppm) and $CDCl_3$ (δ = 77.16 ppm), respectively, as internal standards. Matrix-assisted laser desorption ionization time-of-flight (MALDI-TOF) mass spectra were collected on a Bruker Daltonics Autoflex III spectrometer using dithranol or *trans*-2-[3-(4-*tert*-butylphenyl)-2-methyl-2-propenylidene]malononitrile (DCTB) as matrices. Elemental analyses were carried out with a Yanaco MT-5 analyzer. Thermogravimetric analyses (TGA) were performed using a Hitachi High-Tech Science TG/DTA7300 analyzer at a heating rate of 10 °C min^{-1} under N_2 and 5% weight loss temperatures (T_{d5}) of **1–3** were determined.

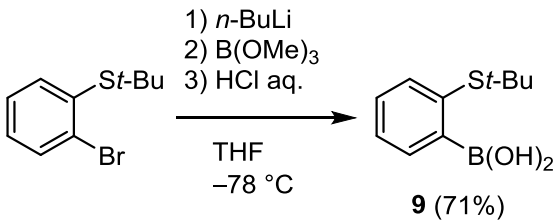

(2-(*tert*-Butylthio)phenyl)boronic acid (9): To a stirred solution of (2-bromophenyl)(*tert*-butyl)sulfane (3.68 g, 15.0 mmol) in anhydrous THF (75 mL) was added *n*-BuLi in hexane (1.6 M, 9.9 mL, 15.8 mmol) at –78 °C. After the reaction mixture was stirred at the same temperature for 30 min, $B(OMe)_3$ (2.6 mL, 23 mmol) was added. The reaction mixture was stirred at the same temperature for 2 h, and then warmed to room temperature. After addition of 2 M aqueous HCl, the product was extracted with ethyl acetate.

The combined organic layer was washed with brine, dried over anhydrous Na_2SO_4, and concentrated under reduced pressure. The crude product was purified by recrystallization from hexane to afford **9** as a white solid (yield = 2.25 g, 10.7 mmol, 71%). ^{1}H NMR (400 MHz, $CDCl_3$): δ 8.46 (s, 1H), 8.12–8.09 (m, 1H), 7.55–7.51 (m, 1H), 7.47–7.40 (m, 2H), 6.56 (s, 2H), 1.30 (s, 9H).

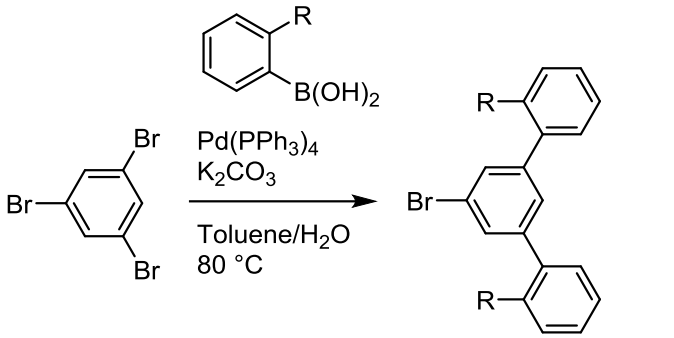

4a: R = OMe (54%)
4b: R = S*t*-Bu (77%)

5'-Bromo-2,2"-dimethoxy-1,1':3'1"-terphenyl (4a): A mixture of 2-methoxyphenylboronic acid (1.83 g, 12.0 mmol), 1,3,5-tribrormobenzene (1.89 g, 6.00 mmol), $Pd(PPh_3)_4$ (136 mg, 0.118 mmol), and K_2CO_3 (3.32 g, 24.0 mmol) in toluene (60 mL) and water (20 mL) was stirred at 80 °C for 24 h. After addition of water, the product was extracted with toluene. The combined organic layer was washed with brine, dried over anhydrous Na_2SO_4, and concentrated under reduced pressure. The crude product was purified by a silica gel column chromatography (eluent: hexane/toluene = 5:1, v/v) to afford **4a** as a colorless sticky oil (yield = 1.19 g, 3.22 mmol, 54%). ^{1}H NMR (400 MHz, $CDCl_3$): δ 7.64 (d, J = 1.6 Hz, 2H), 7.60 (t, J = 1.6 Hz, 1H), 7.36–7.31 (m, 4H), 7.03 (ddd, J = 7.2, 7.2, 1.2 Hz, 2H), 6.90 (dd, J = 8.0, 1.2 Hz, 2H), 3.83 (s, 6H). MS (MALDI-TOF): calcd for $C_{20}H_{17}BrO_2$: 368.04 $[M]^+$; found 367.96.

5'-Bromo-2,2"-di-*tert*-butylthio-1,1':3'1"-terphenyl (4b): A mixture of **9** (2.56 g, 12.2 mmol), 1,3,5-tribrormobenzene (1.91 g, 6.07 mmol), $Pd(PPh_3)_4$ (209 mg, 0.181 mmol), and K_2CO_3 (3.36 g, 24.3 mmol) in toluene (45 mL) and water (15 mL) was stirred at 80 °C for 24 h. After addition of water, the product was extracted with ethyl acetate. The combined organic layer was washed with brine, dried over anhydrous Na_2SO_4, and concentrated under reduced pressure. The crude product was purified by a silica gel column chromatography (eluent: hexane/toluene = 10:1, v/v) to afford **4b** as a white solid (yield = 2.26 g, 4.65 mmol, 77%). ^{1}H NMR (400 MHz, $CDCl_3$): δ 7.70 (d, J = 8.0 Hz, 2H), 7.55 (d, J = 1.6 Hz, 2H), 7.41–7.38 (m, 5H), 7.35–7.30 (m, 2H), 6.90 (dd, J = 8.0, 1.2 Hz, 2H), 1.10 (s, 18H).

10-(2,2”-Dimethoxy-[1,1’:3’1”-terphenyl]-5’-yl)-2,7-dimethyl-10*H*-spiro[acridine-9,9’-fluorene] (6a): A mixture of **4a** (554 mg, 1.50 mmol), **5** (542 mg, 1.50 mmol), $Pd_2(dba)_3$ (29 mg, 0.032 mmol), P(*t*-Bu)$_3$H·BF_4 (36 mg, 0.12 mmol), and sodium *tert*-butoxide (289 mg, 3.01 mmol) in toluene (7.5 mL) was stirred at 100 °C for 20 h. After addition of aqueous solution of NH_4Cl, the product was extracted with toluene. The combined organic layer was washed with brine, dried over anhydrous Na_2SO_4, and concentrated under reduced pressure. The crude product was purified by a silica gel column chromatography (eluent: hexane/toluene = 1:1, v/v) to afford **6a** as a white solid (yield = 809 mg, 1.25 mmol, 83%). ^{1}H NMR (400 MHz, $CDCl_3$): δ 7.87 (t, *J* = 1.6 Hz, 1H), 7.80 (d, *J* = 7.6 Hz, 2H), 7.64 (d, *J* = 1.6 Hz, 2H), 7.49 (dd, *J* = 7.6, 1.6 Hz, 2H), 7.46 (d, *J* = 7.6 Hz, 2H), 7.39–7.33 (m, 4H), 7.24 (ddd, *J* = 7.6, 7.6, 1.6 Hz, 2H), 7.07 (ddd, *J* = 7.6, 7.6, 1.2 Hz, 2H), 7.02 (d, *J* = 8.0 Hz, 2H), 6.77 (ddd, *J* = 8.0, 1.6 Hz, 2H), 6.60 (d, *J* = 8.0 Hz, 2H), 6.18 (d, *J* = 2.0 Hz, 2H), 3.86 (s, 6H), 1.96 (s, 6H). MS (MALDI-TOF): calcd for $C_{47}H_{37}NO_2$: 647.28 $[M]^+$; found 647.52.

10-(2,2”-Di-*tert*-butylthio-[1,1’:3’1”-terphenyl]-5’-yl)-2,7-dimethyl-10*H*-spiro[acridine-9,9’-fluorene] (6b): A mixture of **4b** (1.43 g, 2.95 mmol), **5** (1.12 g, 3.10 mmol), $Pd_2(dba)_3$ (55 mg, 0.060 mmol), P(*t*-Bu)$_3$H·BF_4 (69 mg, 0.24 mmol), and sodium *tert*-butoxide (575 mg, 5.98 mmol) in toluene (15 mL) was stirred at 100 °C for 20 h. After addition of aqueous solution of NH_4Cl, the product was extracted with toluene. The combined organic layer was washed with brine, dried over anhydrous Na_2SO_4, and concentrated under reduced pressure. The crude product was purified by a silica gel column chromatography (eluent: hexane/toluene = 2:1, v/v) to afford **6b** as a white solid (yield = 1.96 g, 2.57 mmol, 87%). ^{1}H NMR (400 MHz, $CDCl_3$): δ 7.80 (d, *J* = 7.6 Hz, 2H), 7.74 (dd, *J* = 7.6, 1.2 Hz, 2H), 7.65 (t, *J* = 1.6 Hz, 1H), 7.57 (dd, *J* = 7.6, 1.6 Hz, 2H), 7.54 (d, *J* = 1.6 Hz, 2H), 7.48–7.43 (m, 4H), 7.38 (dd, *J* = 7.6, 1.2 Hz, 2H), 7.34 (dd, *J* = 7.6, 1.2 Hz, 2H), 7.25 (ddd, *J* = 7.6, 7.6, 1.2 Hz, 2H), 6.73 (dd, *J* = 8.4, 1.6 Hz, 2H), 6.60 (d, *J* = 8.4 Hz, 2H), 6.16 (d, *J* = 2.0 Hz, 2H), 1.95 (s, 6H), 1.17 (s, 18H). MS (MALDI-TOF): calcd for $C_{53}H_{49}NS_2$: 763.33 $[M]^+$; found 763.27.

Compound 1: To a stirred solution of **6a** (648 mg 1.00 mmol) in *o*-dichlorobenzene (5 mL) was added a heptane solution of BBr_3 (1.0 M, 1.0 mL, 1.0 mmol) at 0 °C. After stirring at room temperature for 15 h, *N*,*N*-diisopropylethylamine (0.34 mL, 2.0 mmol) was added to the reaction mixture. After the solvent was removed *in vacuo*, the crude product was washed with hexane and acetonitrile to afford **1** as a white solid (yield = 360 mg, 0.574 mmol, 57%). ^{1}H NMR (400 MHz, $CDCl_3$): δ 8.19 (s, 2H), 8.16 (d, *J* = 7.6 Hz, 2H), 7.85 (d, *J* = 7.2 Hz, 2H),

7.54–7.49 (m, 6H), 7.43 (ddd, J = 7.6, 7.6, 1.2 Hz, 2H), 7.35–7.29 (m, 4H), 6.70 (dd, J = 8.0, 2.0 Hz, 2H), 6.31 (d, J = 8.8 Hz, 2H), 6.23 (d, J = 2.4 Hz, 2H), 1.96 (s, 6H). ^{13}C NMR (100 MHz, $CDCl_3$): δ 156.89, 152.17, 147.65, 143.05, 139.48, 139.26, 130.44, 130.02, 128.59, 128.36, 128.25, 127.71, 126.03, 124.76, 124.54, 123.48, 122.91, 122.83, 120.07, 114.68, 57.06, 20.54. MS (MALDI-TOF): calcd for $C_{45}H_{30}BNO_2$: 627.24 $[M]^+$; found 627.45. Anal. calcd (%) for $C_{45}H_{30}BNO_2$: C 86.13, H 4.82, N 2.23; found: C 86.11, H 4.75, N 2.21. T_{d5}: 405 °C.

Compound 2: To a stirred solution of **6b** (1.15 g 1.50 mmol) in *o*-dichlorobenzene (9 mL) was added a heptane solution of BBr_3 (1.0 M, 1.5 mL, 1.5 mmol) at 0 °C. After stirring at 40 °C for 24 h, *N*,*N*-diisopropylethylamine (0.50 mL, 2.9 mmol) was added to the reaction mixture. After the solvent was removed *in vacuo*, the crude product was washed with hexane and acetonitrile to afford **2** as a yellow solid (yield = 948 mg, 1.44 mmol, 96%). ^{1}H NMR (400 MHz, $CDCl_3$): δ 8.54 (s, 2H), 8.35–7.32 (m, 2H), 7.85 (d, J = 7.2 Hz, 2H), 7.73–7.70 (m, 2H), 7.52 (d, J = 7.6 Hz, 2H), 7.45–7.40 (m, 6H), 7.33 (ddd, J = 7.6, 7.6, 1.2 Hz, 2H), 6.71 (dd, J = 8.4, 1.6 Hz, 2H), 6.34 (d, J = 8.4 Hz, 2H), 6.23 (d, J = 2.0 Hz, 2H), 1.96 (s, 6H). ^{13}C NMR (100 MHz, $CDCl_3$): δ 156.86, 146.19, 142.56, 139.50, 139.21, 132.25, 130.61, 130.11, 128.59, 128.55, 128.40, 128.33, 127.78, 127.73, 127.46, 126.81, 126.05, 124.85, 120.09, 114.66, 57.08, 20.55. MS (MALDI-TOF): calcd for $C_{45}H_{30}BNS_2$: 659.19 $[M]^+$; found 659.13. Anal. calcd (%) for $C_{45}H_{30}BNO_2$: C 81.93, H 4.58, N 2.12; found: C 82.02, H 4.57, N 2.13. T_{d5}: 438 °C.

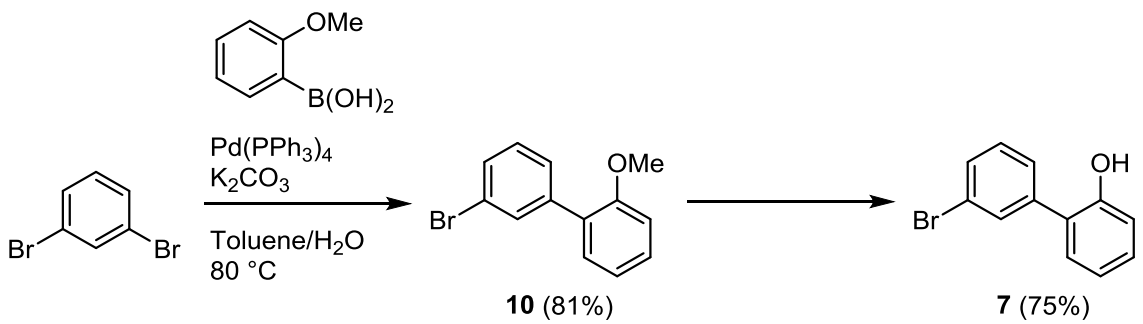

3'-bromo-2-methoxy-1,1'-biphenyl (10): A mixture of 2-methoxyphenylboronic acid (3.95 g, 26.0 mmol), 1,3-dibrormobenzene (9.20 g, 39.0 mmol), $Pd(PPh_3)_4$ (300 mg, 0.260 mmol), and K_2CO_3 10.78 g, 78.0 mmol) in toluene (60 mL) and water (20 mL) was stirred at 80 °C for 24 h. After addition of water, the product was extracted with ethyl acetate. The combined organic layer was washed with brine, dried over anhydrous Na_2SO_4, and concentrated under reduced pressure. The crude product was purified by a silica gel column chromatography (eluent:

hexane) to afford **10** as a colorless oil (yield = 5.56 g, 21.1 mmol, 81%). ^{1}H NMR (400 MHz, $CDCl_3$): δ 7.68 (dd, J = 2, 2 Hz, 1H), 7.46–7.43 (m, 2H), 7.36–7.31 (m, 1H), 7.30–7.24 (m, 2H), 7.02 (ddd, J = 7.6, 7.6, 1.2 Hz, 1H), 6.98 (dd, J = 8.0, 1.2 Hz, 1H), 3.82 (s, 3H).

3'-bromo-[1,1'-biphenyl]-2-ol (7): To a stirred solution of **10** (5.28 g 20.1 mmol) in anhydrous CH_2Cl_2 (40 mL) was added a heptane solution of BBr_3 (1.0 M, 24 mL, 24 mmol) at 0 °C. After stirring at room temperature for 19 h, water was added to the reaction mixture. The product was extracted with CH_2Cl_2. The combined organic layer was washed with brine, dried over anhydrous Na_2SO_4, and concentrated under reduced pressure. The crude product was purified by a silica gel column chromatography (eluent: hexane/ethyl acetate = 5:1, v/v) to afford **7** as a white solid (yield = 3.75 g, 15.0 mmol, 75%). ^{1}H NMR (400 MHz, $CDCl_3$): δ 7.65 (dd, J = 1.6, 1.6 Hz, 1H), 7.53 (ddd, J = 8.0, 2.0, 1.2 Hz, 1H), 7.43 (ddd, J = 8.0, 1.6, 1.6 Hz, 1H), 7.35 (dd, J = 8.0, 8.0 Hz, 1H), 7.30–7.21 (m, 2H), 7.00 (ddd, J = 7.6, 7.6, 1.2 Hz, 1H), 6.96 (dd, J = 8.0, 1.2 Hz, 1H), 5.04 (s, 1H).

6-Bromo-9-methoxy-10,9-oxaboraphenanthrene (8): A heptane solution of BCl_3 (1.0 M, 6.0 mL, 6.0 mmol) was added to an anhydrous toluene (30 mL). A solution of **7** (996 mg, 4.00 mmol) dissolved in anhydrous toluene (8 mL) was added dropwise at 0 °C. After the reaction mixture was warmed to room temperature, $AlCl_3$ (60 mg, 0.45 mmol) was added. After stirring at 120 °C for 15 h, methanol (4 mL) was added to the reaction mixture at 0 °C. After the solvent was removed *in vacuo*, the crude product was dissolved in anhydrous CH_2Cl_2 and filtered. After the filtrate was concentrated under reduced pressure, the crude product was washed with methanol to afford the 10,9-oxaboraphenanthrene intermediate as a brown solid. The obtained intermediate was used for the next reaction without further purification.

To a stirred solution of 1-bromo-2,4,6-triisopropylbenzene (1.14 g, 4.02 mmol) in anhydrous THF (20 mL) was added *n*-BuLi in hexane (1.57 M, 2.57 mL, 4.03 mmol) at –78 °C. After the reaction mixture was stirred at the same temperature for 1 h, the intermediate dissolved in anhydrous THF (10 mL) was added. After the reaction mixture was warmed to 0 °C and then gradually warmed to room temperature. After addition of water, the product was extracted with ethyl acetate. The combined organic layer was washed with brine, dried over anhydrous Na_2SO_4, and concentrated under reduced pressure. The crude product was purified by a silica gel column chromatography (eluent: hexane/toluene = 4:1, v/v) and then reprecipitated from hexane/ethanol to afford **8** as a white solid (yield = 528 mg, 1.14 mmol, 29%). ^{1}H NMR (400 MHz, $CDCl_3$): δ 8.46 (s, 1H), 8.24 (d, J = 7.6 Hz, 1H), 7.69 (d, J = 8.4 Hz, 1H), 7.56–7.51 (m, 3H), 7.07 (s, 2H), 2.96 (sept, J = 6.4 Hz, 1H), 2.54 (sept, J = 6.4 Hz,

2H), 1.32 (d, J = 7.2 Hz, 6H), 1.19 (d, J = 6.8 Hz, 6H), 1.08 (d, J = 6.8 Hz, 6H). MS (MALDI-TOF): calcd for $C_{27}H_{30}BBrO$: 460.16 $[M]^+$; found 460.20.

Compound 3: A mixture of **8** (162 mg, 0.351 mmol), **5** (127 mg, 0.351 mmol), $Pd_2(dba)_3$ (6.8 mg, 0.0076 mmol), P(*t*-Bu)$_3$H·BF_4 (8.9 mg, 0.031 mmol), and sodium *tert*-butoxide (51 mg, 0.531 mmol) in toluene (3.5 mL) was stirred at 90 °C for 16 h. After addition of water, the product was extracted with toluene. The combined organic layer was washed with brine, dried over anhydrous Na_2SO_4, and concentrated under reduced pressure. The crude product was purified by a silica gel column chromatography (eluent: hexane/toluene = 3:1, v/v) and then reprecipitated from CH_2Cl_2/methanol to afford **3** as a white solid (yield = 169 mg, 0.228 mmol, 65%). ^{1}H NMR (400 MHz, $CDCl_3$): δ 8.43 (s, 1H), 8.29 (d, J = 8.0 Hz, 1H), 8.15 (d, J = 8.4 Hz, 1H), 7.83 (d, J = 7.6 Hz, 2H), 7.60–7.36 (m, 8H), 7.29 (d, J = 7.6 Hz, 2H), 7.13 (s, 2H), 6.72 (d, J = 8.4 Hz, 2H), 6.30 (d, J = 8.4 Hz, 2H), 6.21 (s, 2H), 2.99 (sept, J = 6.4 Hz, 1H), 2.71 (sept, J = 6.4 Hz, 2H), 1.95 (s, 6H), 1.35 (d, J = 6.8 Hz, 6H), 1.28 (d, J = 6.4 Hz, 6H), 1.19 (d, J = 6.4 Hz, 6H). ^{13}C NMR (100 MHz, $CDCl_3$): δ 156.69, 151.94, 151.54, 149.86, 146.40, 141.09, 140.74, 139.45, 139.24, 129.96, 129.88, 129.80, 128.55, 128.19, 127.67, 125.98, 124.90, 124.67, 123.96, 123.72, 122.82, 121.00, 120.49, 120.03, 114.62, 57.08, 35.45, 34.68, 25.16, 24.27, 24.22, 20.54. MS (MALDI-TOF): calcd for $C_{27}H_{30}BBrO$: 739.40 $[M]^+$; found 739.45. Anal. calcd (%) for $C_{54}H_{50}BNO$: C 87.67, H 6.81, N 1.89; found: C 87.65, H 6.84, N 1.87. T_{d5}: 369 °C.

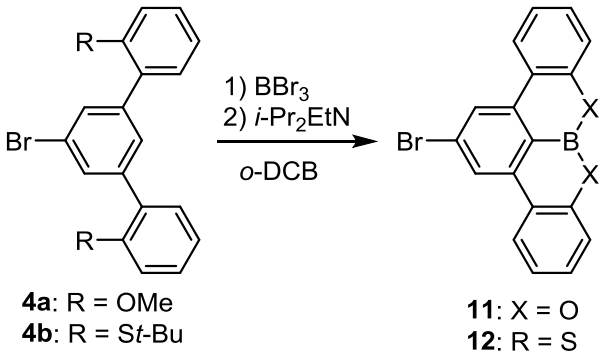

2-Bromo-8,9-dioxa-8a-borabenzo[*fg*]tetracene (11): To a stirred solution of **4a** (560 mg 1.52 mmol) in *o*-dichlorobenzene (6 mL) was added a heptane solution of BBr_3 (1.0 M, 1.5 mL, 1.5 mmol) at 0 °C. After stirring at room temperature for 18 h, *N*,*N*-diisopropylethylamine (0.80 mL, 4.7 mmol) was added to the reaction mixture at 0 °C. After stirring at 180 °C for 24 h, the reaction mixture was cooled to room temperature. After addition of chloroform, the reaction mixture was filtered through a Celite® pad. The filtrate

was washed with water and brine, dried over anhydrous Na_2SO_4, and concentrated under reduced pressure. The crude product was purified by a silica gel column chromatography (eluent: chloroform) and then washed with hexane to afford **11** as a white solid (yield = 292 mg, 0.837 mmol, 55%). ^{1}H NMR (400 MHz, $CDCl_3$): δ 8.21 (s, 2H), 8.08 (d, J = 7.6 Hz, 2H), 7.50–7.43 (m, 4H), 7.29 (m, 2H). MS (MALDI-TOF): calcd for $C_{18}H_{10}BBrO_2$: 348.00 $[M]^+$; found 347.96.

2-Bromo-8,9-dithia-8a-borabenzo[*fg*]tetracene (12): To a stirred solution of **4b** (215 mg 0.443 mmol) in *o*-dichlorobenzene (2 mL) was added a heptane solution of BBr_3 (1.0 M, 0.45 mL, 0.45 mmol) at 0 °C. After stirring at 40 °C for 24 h, *N*,*N*-diisopropylethylamine (0.26 mL, 1.5 mmol) was added to the reaction mixture at room temperature. After stirring at 180 °C for 24 h, the reaction mixture was cooled to room temperature. After the solvent was removed *in vacuo*, the crude product was washed with hexane. The crude crude product was purified by temperature-gradient vacuum sublimation to afford **12** as a white solid (yield = 59 mg, 0.15 mmol, 34%). ^{1}H NMR (400 MHz, $CDCl_3$): δ 8.53 (s, 2H), 8.27 (d, J = 8.0 Hz, 2H), 8.65 (d, J = 8.0 Hz, 2H), 7.46–7.38 (m, 4H). MS (MALDI-TOF): calcd for $C_{18}H_{10}BBrS_2$: 379.95 $[M]^+$; found 379.77.

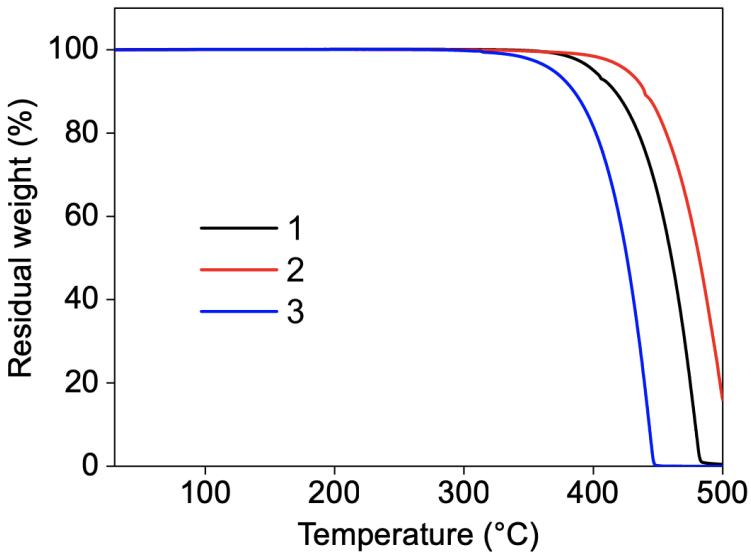

Fig. S1 TGA thermograms of **1–3** at a heating rate of 10 °C min^{-1} under N_2.

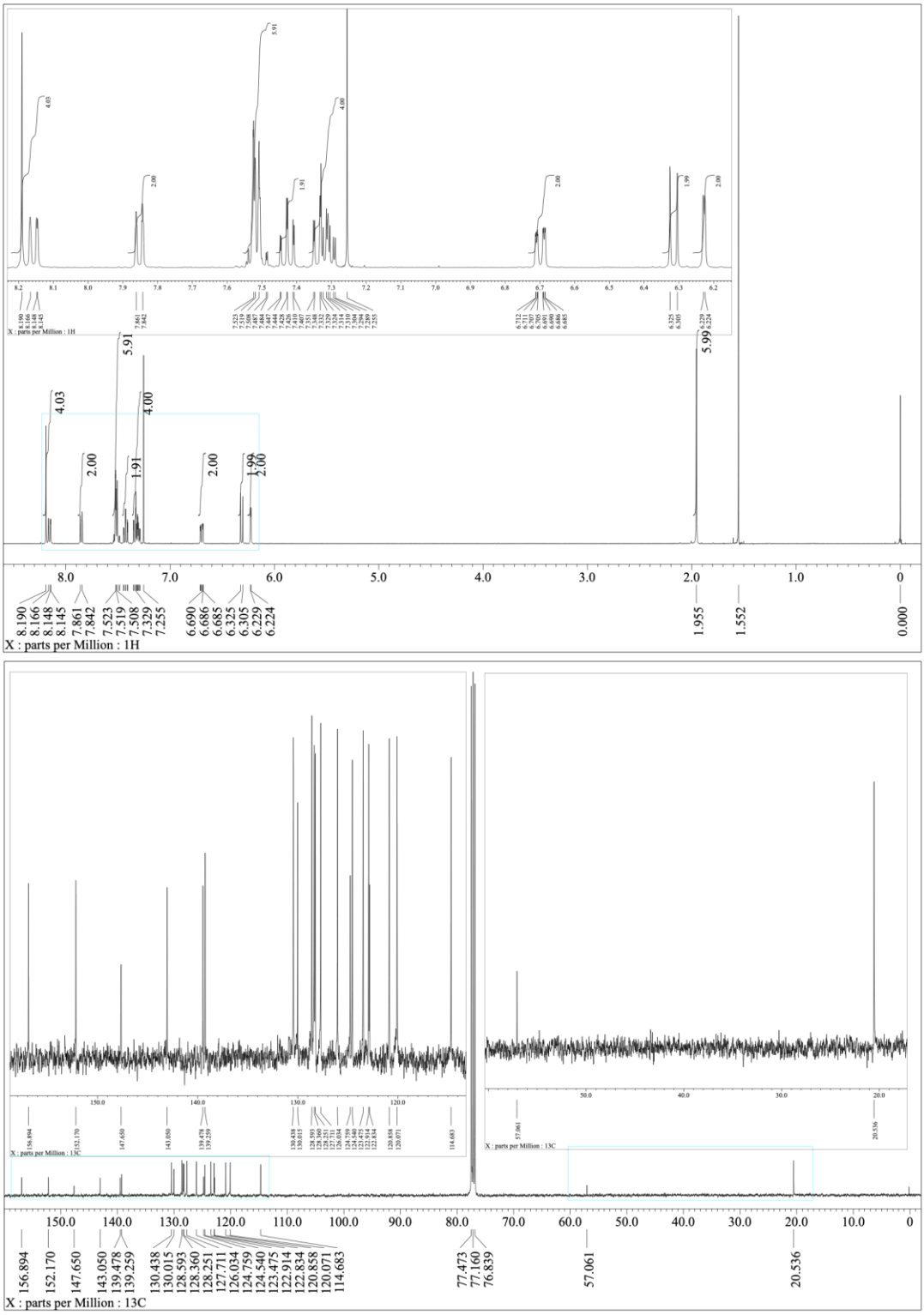

Fig. S2 ^{1}H and ^{13}C NMR spectra of **1** in $CDCl_3$.

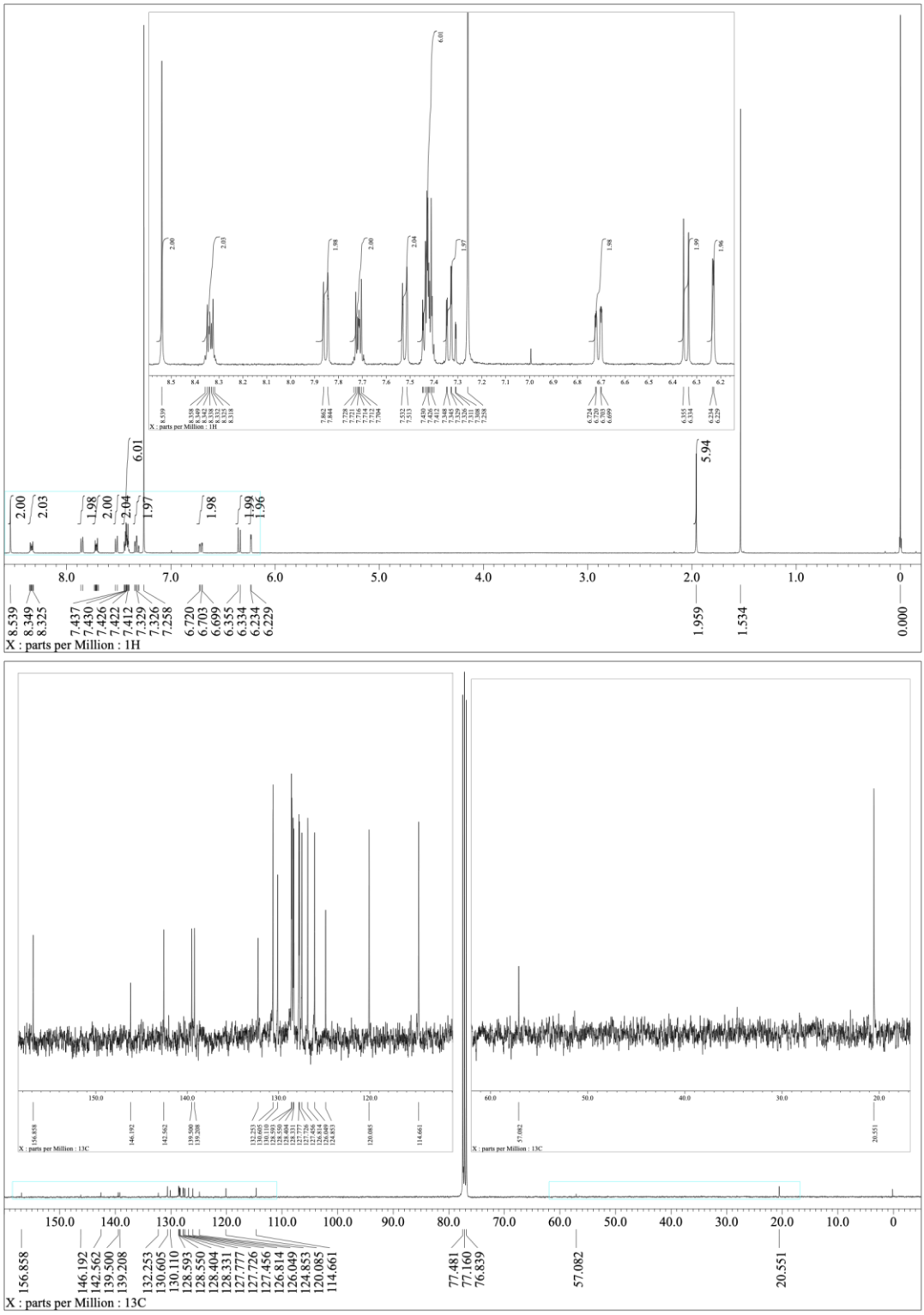

Fig. S3 ^{1}H and ^{13}C NMR spectra of **2** in $CDCl_3$.

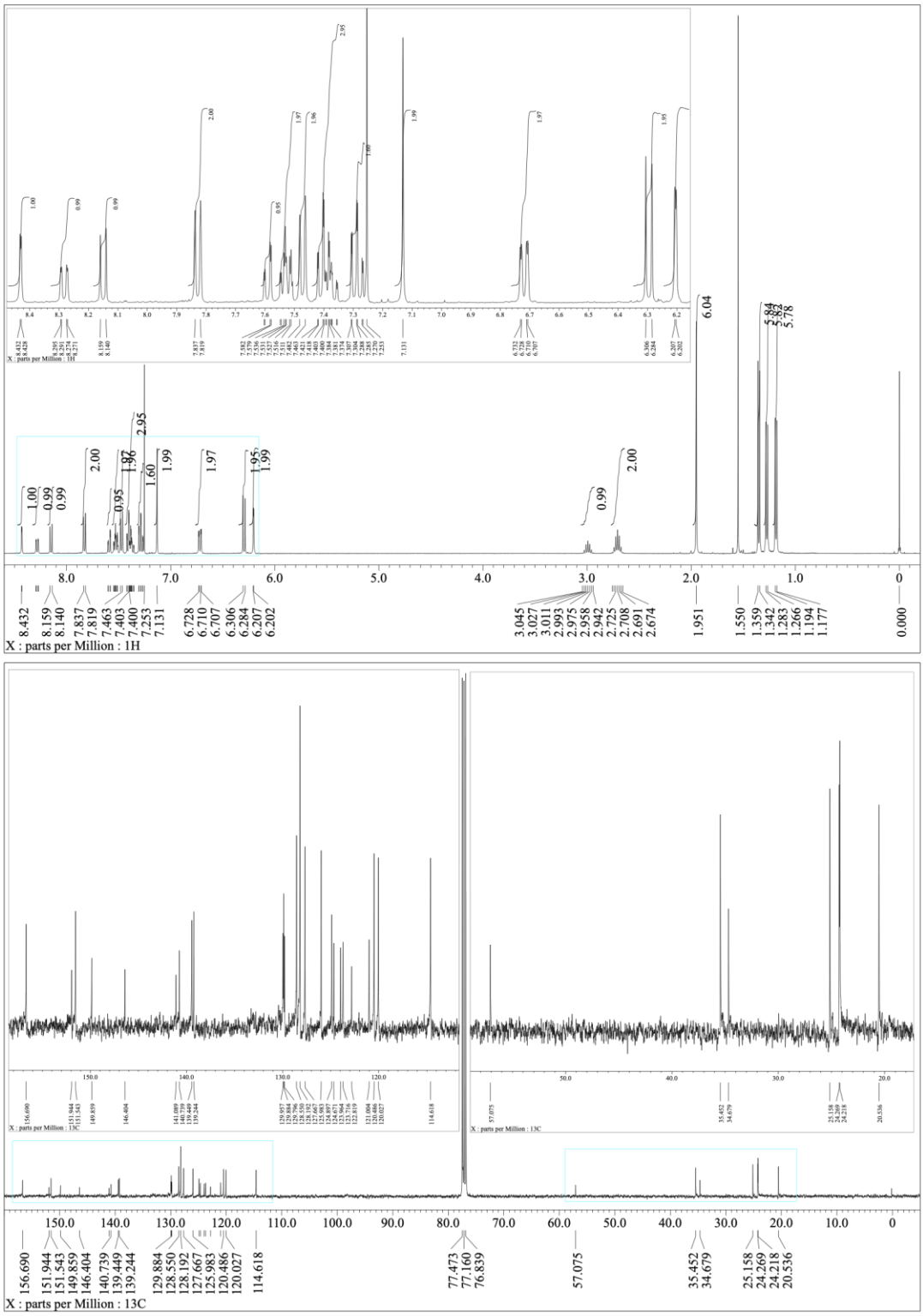

Fig. S4 ^{1}H and ^{13}C NMR spectra of **3** in $CDCl_3$.

2. X-ray Crystallographic Analysis

Single crystal X-ray diffraction measurements were performed on a Rigaku Saturn724+ diffractometer with multi-layer mirror monochromated Mo-Kα radiation. The structures were solved by direct methods (SHELXT-2016[6]) and refined by the full-matrix least-squares on F^2 (SHELXL-2016[6]). All non-hydrogen atoms were refined anisotropically. All hydrogen atoms were placed using AFIX instructions.

Crystallographic data for 1: Colorless block crytsals of **1** were obtained by the recrystallization from chloroform and methanol using a vapor diffusion method. The measurement was performed at 159 K. Total 56298 reflections were collected, among which 11943 reflections were independent (R_{int} = 0.0699). The crystal data: Formula $2(C_{45}H_{30}BNO_2)\cdot(CHCl_3)$; FW = 1374.38, crystal size 0.20 × 0.15 × 0.15 mm, Monoclinic, $P2_1/c$ (#14), a = 13.346(6), b = 19.308(8), c = 27.053(11) Å, $\alpha = \gamma = 90°$, β = 101.308(8)°, V = 6832(5) Å^3, Z = 4, D_{calcd} = 1.336 g cm^{-3}, R_1 = 0.0664 ($I > 2\sigma(I)$), wR_2 = 0.2150 (all data), GOF = 1.056. Two crystallographically independent **1** and one chloroform molecule used as solvent were contained in an asymmetric unit of the crystal lattice. The dihedral angle between the donor and acceptor units of **1** described in the manuscript (84.9°) is the value of one molecule. The value of the other molecule is 81.4°. The crystal data is deposited in The Cambridge Crystallographic Data Centre (CCDC number: 1873221).

Crystallographic data for 2: Yellow block crytsals of **2** were obtained by the recrystallization from chloroform and acetonitrile using a vapor diffusion method. The measurement was performed at 159 K. Total 27061 reflections were collected, among which 5828 reflections were independent (R_{int} = 0.0775). The crystal data: Formula $C_{45}H_{30}BNS_2$; FW = 659.63, crystal size 0.22 × 0.18 × 0.10 mm, Monoclinic, $P2_1/n$ (#14), a = 9.425(5), b = 28.656(14), c = 12.602(6) Å, $\alpha = \gamma = 90°$, β = 102.554(6)°, V = 3322(3) Å^3, Z = 4, D_{calcd} = 1.319 g cm^{-3}, R_1 = 0.0590 ($I > 2\sigma(I)$), wR_2 = 0.1440 (all data), GOF = 1.077. The crystal data is deposited in The Cambridge Crystallographic Data Centre (CCDC number: 1873222).

Crystallographic data for 3: Colorless platelet crytsals of **3** were obtained by the recrystallization from ethyl acetate and methanol using a vapor diffusion method. The measurement was performed at 123 K. Total 38860 reflections were collected, among which 8489 reflections were independent (R_{int} = 0.0693). The crystal data: Formula $C_{54}H_{50}BNO\cdot C_4H_8O_2$; FW = 827.86, crystal size 0.10 × 0.08 × 0.04 mm, Orthorhombic, $Pna2_1$ (#33), a = 19.767(13), b = 24.550(16), c = 9.996(6) Å, $\alpha = \beta = \gamma = 90°$, V = 4851(5) Å^3, Z = 4,

D_{calcd} = 1.134 g cm^{-3}, R_1 = 0.0732 ($I > 2\sigma(I)$), wR_2 = 0.2221 (all data), GOF = 1.060. One ethyl acetate molecule used as solvent was contained in an asymmetric unit of the crystal lattice. The crystal data is deposited in The Cambridge Crystallographic Data Centre (CCDC number: 1873223).

3. Photophysical Properties

UV-vis absorption spectra were measured with a Jasco V-670 spectrometer. Fluorescence and phosphorescence spectra were measured with a Jasco FP-8600 spectrophotometer. Absolute photoluminescence quantum yields (Φ_{PL}) were determined with a Jasco ILF-835 integrating sphere system. The transient PL decay measrurements were performed using a Quantaurus-Tau C11367 under N_2. Photophysical properties of **1–3** in toluene solutions were measured by using deoxygenated spectral grade solvents in the concentration of 4~6 × 10^{-5} M. Pure neat films for the optical measurements were deposited under high vacuum (< 1 × 10^{-4} Pa) onto quartz substrates. The optical energy gaps (E_g) were determined from the high energy onset position of the UV-vis absorption spectra of pure neat films. The ionization potential (E_{IP}) were determined from the high energy onset position of the photoelectron yield spectra of pure neat films. The electron affinities (E_{EA}) were estimated by subtracting E_g from the measured E_{IP}. The 20 wt%-doped films for the optical measurements were co-deposited with PPF as a host material under high vacuum (< 1 × 10^{-4} Pa) onto quartz substrates. The singlet (E_S) and triplet excitation energies (E_T) were estimated from the high energy onset position of the fluorescence and phosphorescence spectra of the 20 wt%-doped films. The rate constants for the TADF decay process of **1–3** were calculated according to the literature.[7]

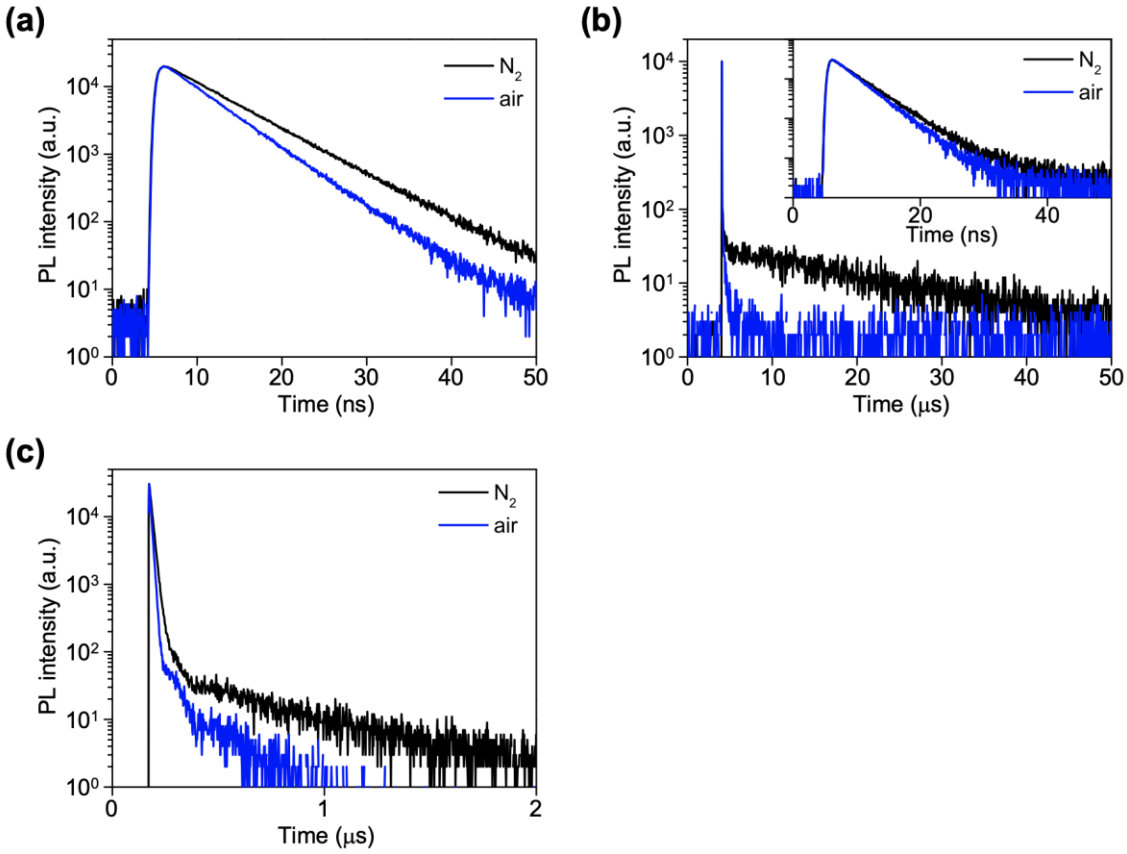

Fig. S5 Transient PL decays of (a) **1**, (b) **2**, and (c) **3** in deoxygenated (black line) and aerated (blue line) toluene solutions at 300 K.

Table S1 Photophysical Data Measured in Toluene Solutions.

	λ_{abs} [nm]	λ_{PL} [nm]	λ_{FWHM} [nm] ([eV])	Φ_{PL} [%]	τ_p [ns]	τ_d [μs]
1	376	462	77 (0.44)	11	6.3	-
2	406	483	75 (0.39)	4	4.0	18
3	384	448	67 (0.40)	21	15	0.31

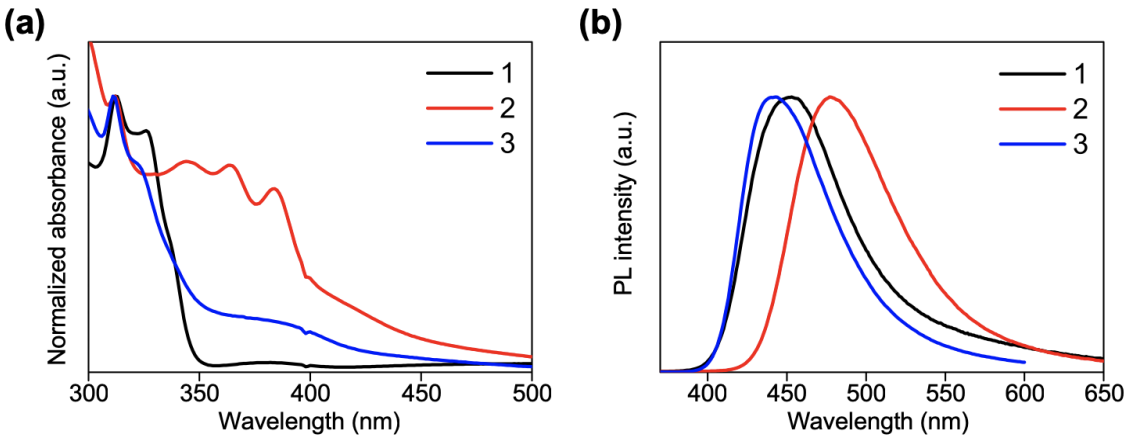

Fig. S6 (a) UV-vis absorption and (b) PL spectra of **1–3** in pure neat films.

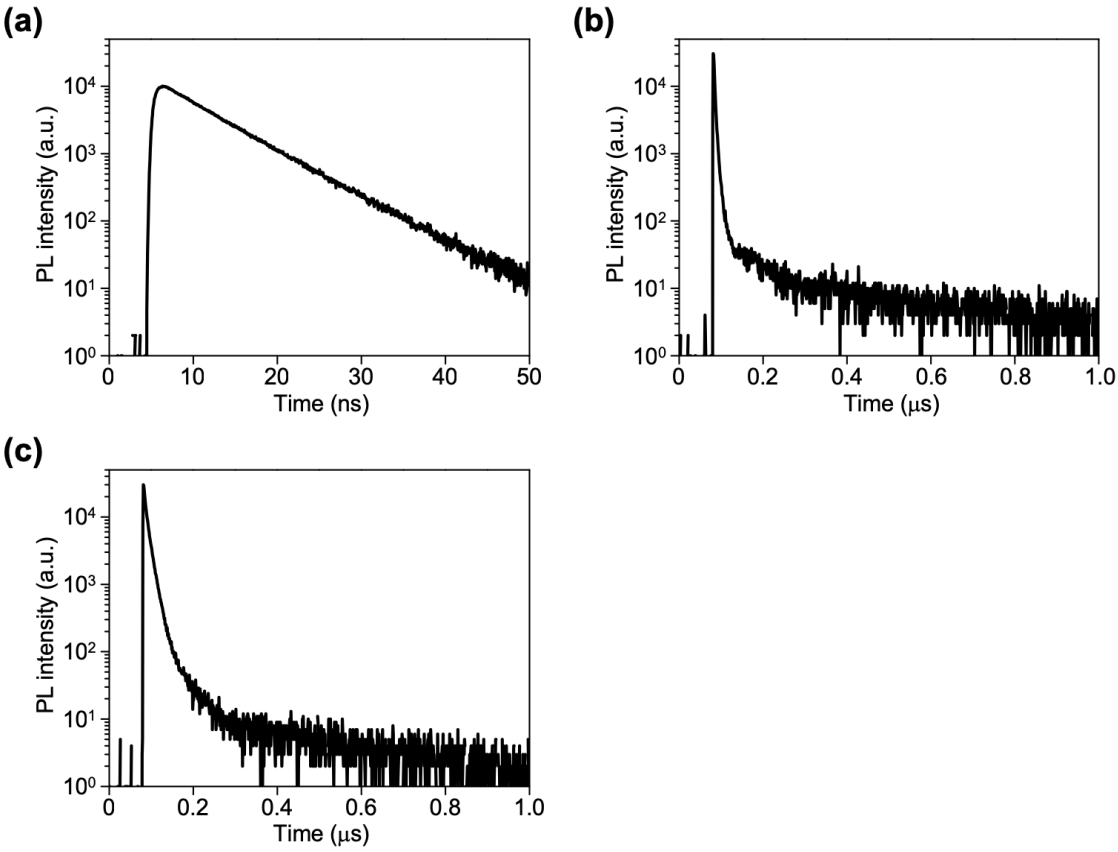

Fig. S7 Transient PL decays of (a) **1**, (b) **2**, and (c) **3** in pure neat films under N_2 at 300 K.

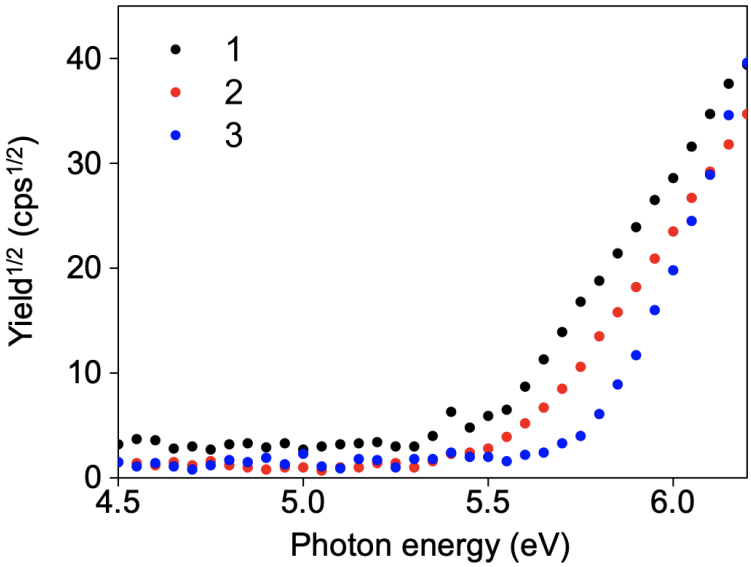

Fig. S8 Photoelectron yield spectra of **1–3** in pure neat films.

Table S2 Photophysical Data Measured in Pure Neat Films.

	λ_{abs} (onset) [nm]	λ_{PL} [nm]	λ_{FWHM} [nm] ([eV])	Φ_{PL} [%]	τ_p [ns]	τ_d [μs]	E_g [eV]	E_{IP} [eV]	E_{EA} [eV]
1	412	453	73 (0.43)	4	6.1	-	3.01	5.49	2.48
2	450	477	76 (0.40)	10	3.1	0.067	2.75	5.58	2.83
3	422	443	66 (0.40)	13	4.6	0.014	2.94	5.80	2.86

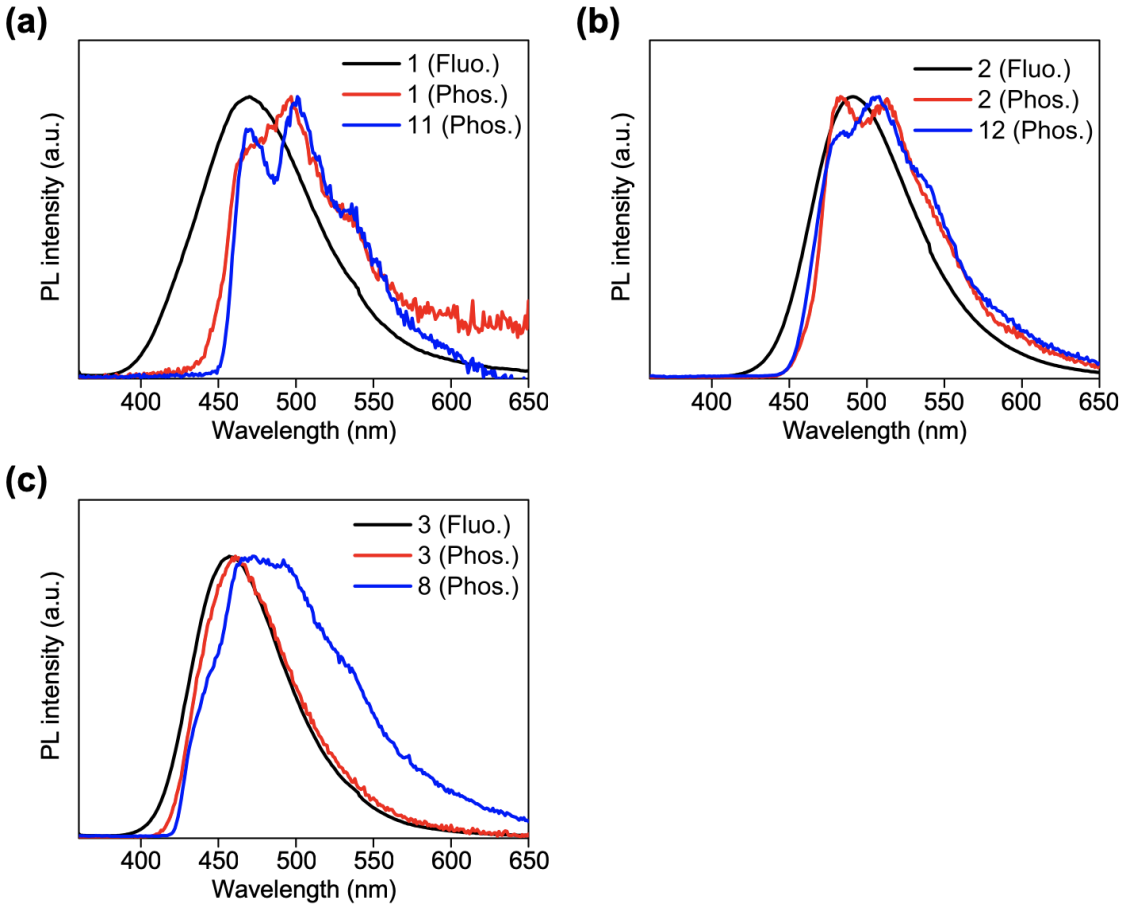

Fig. S9 Fluorescence (300 K) and phosphorescence (123 K) spectra of **1**–**3**, **11**, **12**, and **8** in 20 wt%-doped thin films in PPF under N_2. The E_T values of **11**, **12**, and **8** were calculated to be 2.74, 2.74, and 2.94 eV, respectively.

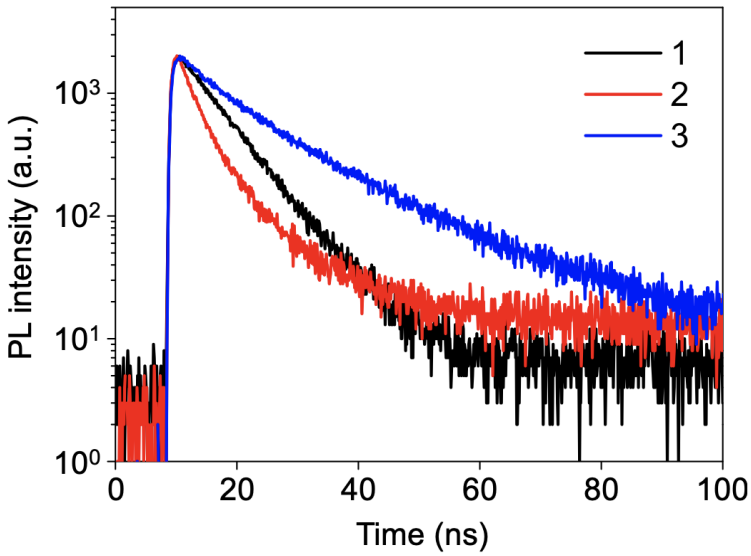

Fig. S10 Nanosecond-order transient PL decays of the 20 wt%-doped films of **1**–**3** in PPF under N_2 at 300 K.

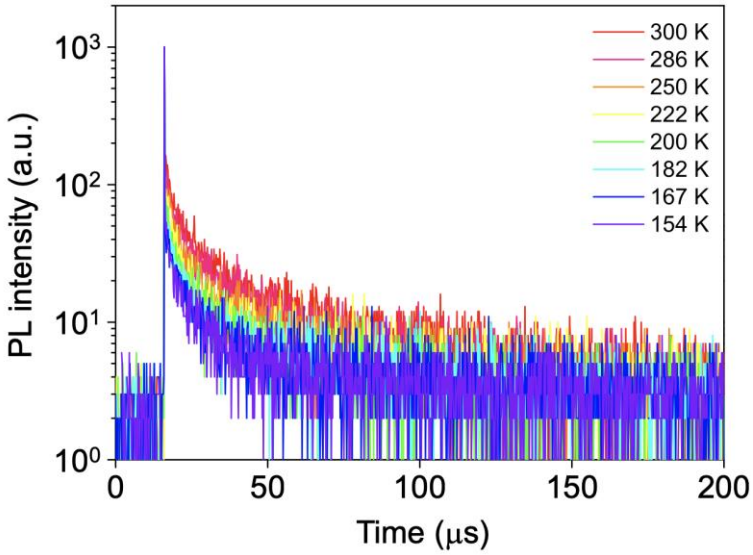

Fig. S11 Temperature dependence of transient PL decay of the 20 wt%-doped film of **2** in PPF under N_2 in the temperature range of 154–300 K.

Table S3 Photophysical Data Measured in a PPF host matrix.

	λ_{PL} [nm]	λ_{FWHM} [nm] ([eV])	Φ_{PL} [%]	Φ_p [%]	Φ_d [%]	τ_p [ns]	τ_d [μs]
1	470	89 (0.49)	28	0.6	27	6.9	140
2	491	77 (0.39)	81	1.2	80	4.5	22
3	458	75 (0.43)	53	5.4	48	14	12

Table S4 The Rate Constants and Quantum Efficiencies for Decay Processes in the 20wt%-Doped Films in a PPF Host.

	k_r^S [10^6 s^{-1}]	k_{ISC} [10^7 s^{-1}]	k_{RISC} [10^5 s^{-1}]	K_{nr}^T [10^3 s^{-1}]	Φ_{ISC} [%]	Φ_{RISC} [%]
1	0.83	14	3.5	5.3	99	99
2	2.6	22	32	8.7	99	99.7
3	4.0	7.0	8.1	43	95	95

4. Computational Method

Geometry optimization in the S_0 state of **1–3** were performed using the B3LYP functional with the 6-31G(d) basis set in the gas phase, implemented in the Gaussian 16 program package.[8] The geometries of the S_1 and T_1 states were optimized using the TD-DFT method at the M062X/6-31G(d) level in the gas phase. The singlet and triplet excitation energies were calculated by TD-DFT calculations using the optimally tuned range-separated functional (LC-ωPBE) with the 6-31+G(d) basis set. The optimal range-separation parameter ω was obtained by minimizing the following equation,[9]

$$J^2 = \sum_{i=0}^{1} [\varepsilon_{HOMO}(N+i) + IP(N+i)]^2$$

where ε_{HOMO} is the energy of the HOMO and *IP* is the ionization potential for the *N*-electron system. For the optimization of the ω value, the single-point calculations based on the S_0 geometries optimized at B3LYP/6-31G(d) level were carried out for **1** and **3**. The optimal ω value of 0.155 was used in the all TD-DFT LC-ωPBE calculations for **1–3** in the S_0, S_1 and T_1 optimized geometries.

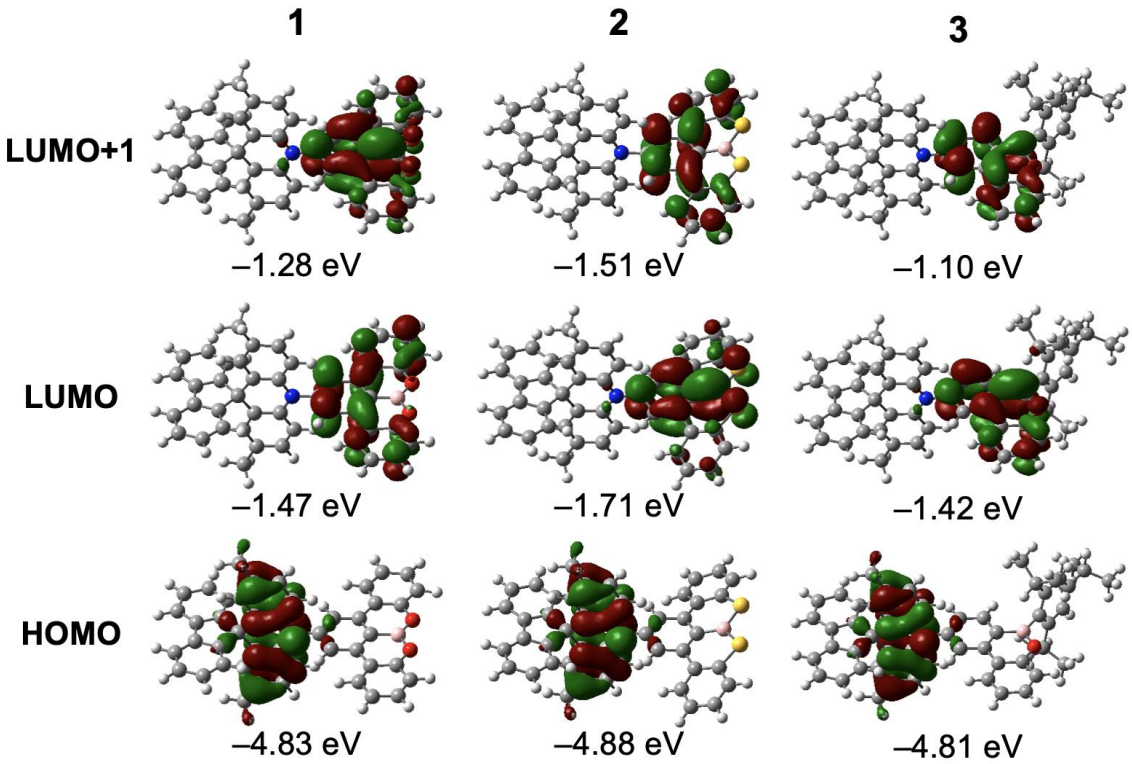

Fig. S12 Kohn–Sham molecular orbitals of **1–3** in the S_0 states and their energy levels, calculated at the B3LYP/6-31G(d) level.

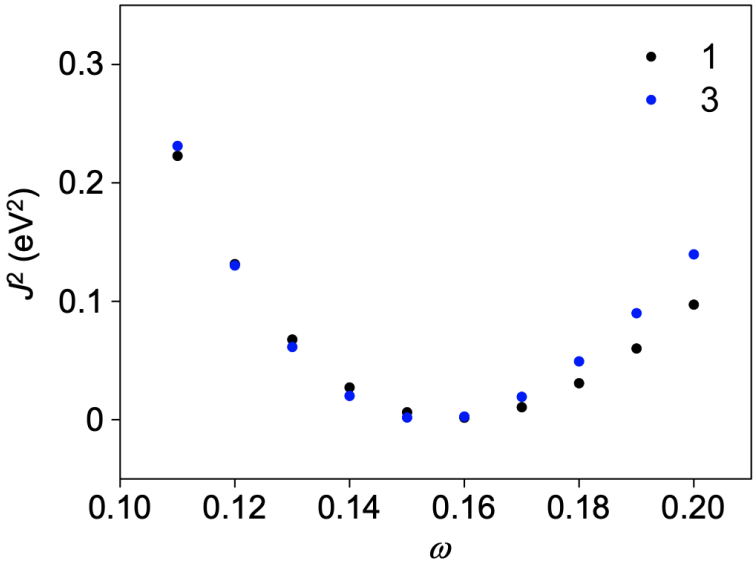

Fig. S13 J^2 values as a function of the range-separation parameter ω for **1** and **3** calculated at the LC-ωPBE/6-31+G(d) level.

Table S5 TD-DFT Calculation Results in the S_0 Optimized Geometries.

The excitation energies (E), oscillator strength (f), transition configurations, and singlet–triplet energy splittings (ΔE_{ST}) of **1–3** calculated at the LC-ωPBE/6-31+G(d) level in the S_0 optimized geometries.

	state	E [eV]	f	main configuration [%]		ΔE_{ST} [meV]
1	S_1	3.049	0.0007	H → L	96	164
	T_1	2.885	0.0000	H–2 → L	70	
				H–8 → L+1	9	
				H–7 → L	9	
2	S_1	2.917	0.0000	H → L	94	52
	T_1	2.865	0.0000	H−1 → L+1	52	
				H−4 → L+1	11	
				H−6 → L+1	9	
3	S_1	3.052	0.0000	H → L	75	16
				H → L+1	18	
	T_1	3.036	0.0000	H → L	71	
				H → L+1	22	

H−n → L+m represents the HOMO−n to LUMO+m transition.

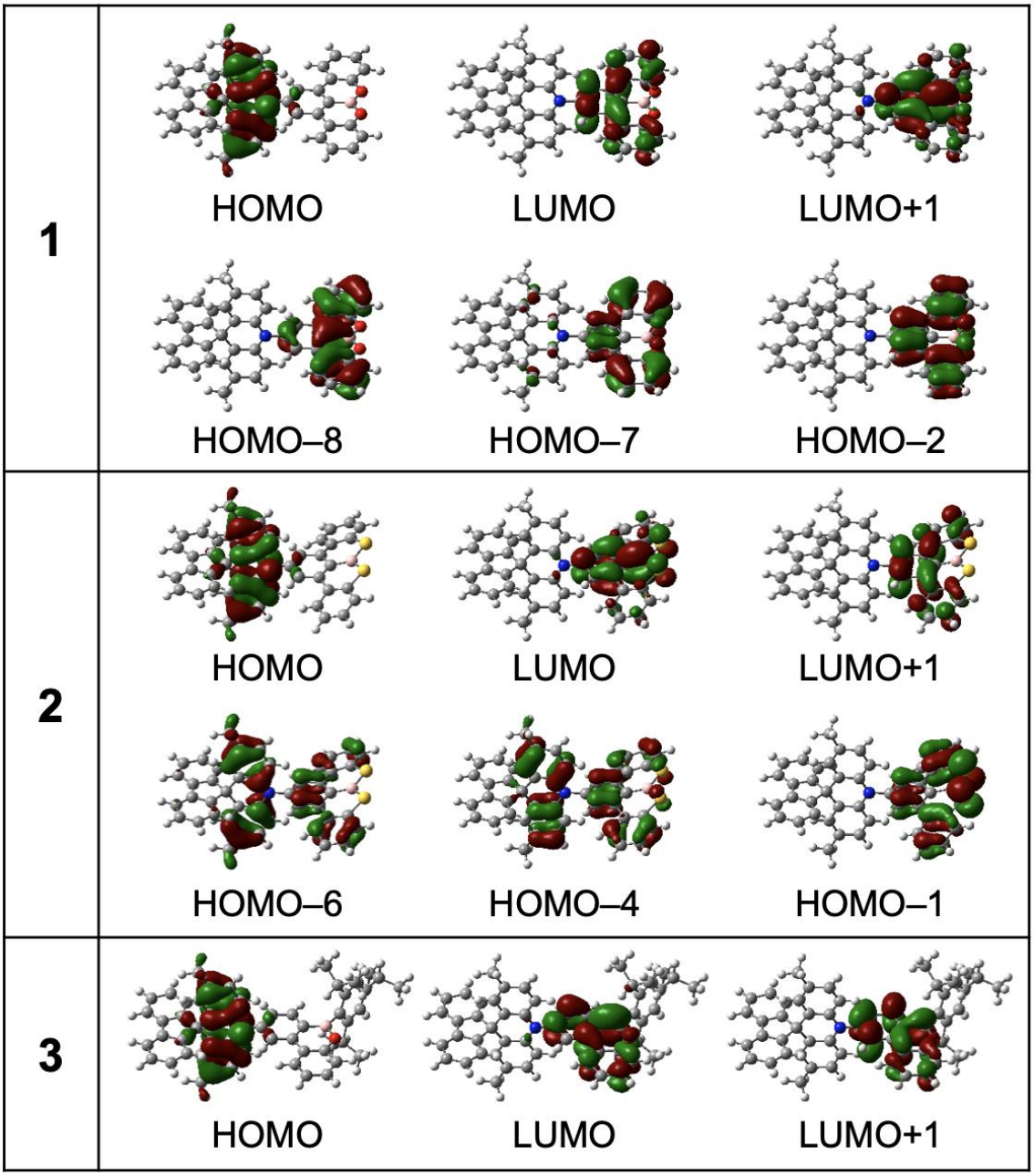

Fig. S14 Kohn–Sham molecular orbitals of **1–3** most involved in the vertical excitations for the S_1 and T_1 states, calculated at the LC-ωPBE/6-31+G(d) level in the S_0 optimized geometries.

Table S6 TD-DFT Calculation Results in the S_1 and T_1 Optimized Geometries.

The excitation energies (E), relaxation energies (λ), the energy levels of the excited states (Es and E_T), f, transition configurations, and adiabatic ΔE_{ST} of **1–3** calculated at the LC-ωPBE/6-31+G(d) level in the S_1 and T_1 optimized geometries. E_S (E_T) = $E + \lambda$.

	state	E [eV]	λ [eV]	E_S, E_T [eV]	f	main configuration [%]		ΔE_{ST} [meV]
1	S_1	2.762	0.248	3.010	0.0000	H → L	93	309
	T_1	2.312	0.389	2.701	0.0000	H−1 → L	85	
2	S_1	2.490	0.299	2.789	0.0000	H → L	95	140
	T_1	2.214	0.435	2.649	0.0000	H−1 → L	76	
3	S_1	2.642	0.337	2.979	0.0002	H → L	91	88
	T_1	2.422	0.468	2.890	0.0000	H → L	77	

H−n → L+m represents the HOMO−n to LUMO+m transition.

5. OLED Fabrication and Characterization

Indium tin oxide-coated glass substrates were cleaned with detergent, deionized water, acetone, and isopropanol. They were then treated with UV–ozone treatment for 30 min, before being loaded into a vacuum evaporation system. The organic layers were thermally evaporated on the substrates under vacuum (< 1 × 10^{-4} Pa) with an evaporation rate of < 1 Å/s. All of the layers were deposited through a shadow mask. The layer thickness and deposition rate were monitored *in situ* during deposition by an oscillating quartz thickness monitor. OLED properties were measured using a Keithley source meter 2400 and a Konica Minolta CS-2000.

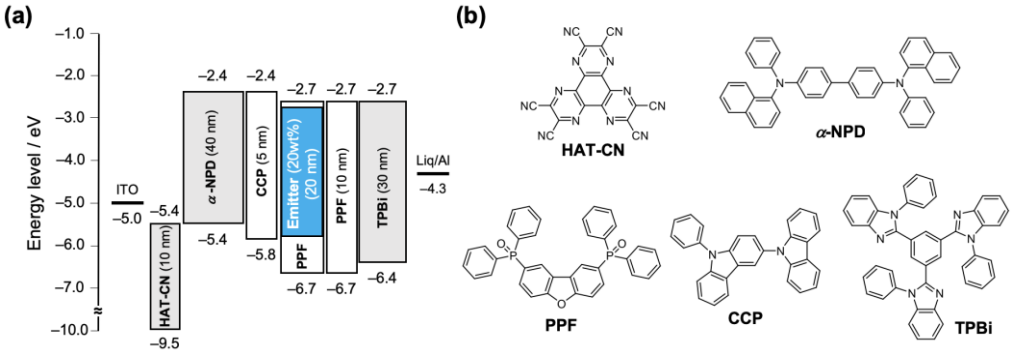

Fig. S15 (a) Schematic energy-level diagram for OLED based on **1–3** as emitters and (b) molecular structures of the materials used in the devices.

Table S7 The EL Performance of the OLEDs Based on 1–3.

	λ_{EL} [nm]	λ_{FWHM} [nm] ([eV])	CIE (x, y)	V_{on} [V]	η_{ext} [%] Max / 100 / 500 / 1000 cd m^{-2}	η_c [cd A^{-1}]	η_p [lm W^{-1}]
1	471	80 (0.43)	(0.16, 0.22)	3.8	5.2 / 1.3 / 0.39 / -	9.1	7.5
2	489	71 (0.36)	(0.17, 0.39)	3.6	20.9 / 17.5 / 12.1 / 9.2	46.7	40.7
3	462	67 (0.38)	(0.15, 0.15)	4.0	12.8 / 5.9 / 1.5 / -	16.1	12.4

[a]Abbreviations: λ_{EL} = EL emission maximum, λ_{FWHM} = Full width at half-maximum of the EL spectrum, CIE = Commission Internationale de l'Éclairage color coordinates, V_{on} = turn-on voltage at 1 cd m^{-2}, η_{ext} = maximum external EL quantum efficiency, η_c = maximum current efficiency, η_p = maximum power efficiency.

6. References

1. S. B. Harkins and J. C. Peteres, *J. Am. Chem. Soc.*, 2004, **126**, 2885.

2. R. Shukla, S. V. Lindeman and R. Rathore, *Chem. Commun.*, 2009, 5600.

3. I. S. Park, M. Numata, C. Adachi and T. Yasuda, *Bull. Chem. Soc. Jpn.*, 2016, **89**, 375.

4. P. A. Vecchi,A. B. Padmaperuma, H. Qiao, L. S. Sapochak and P. E. A. Burrows, *Org. Lett.*, 2006, **8**, 4211.

5. H. Wang, L. Xie, Q. Peng, L. Meng, Y. Wang, Y. Yi and P. Wang, *Adv. Mater.*, 2014, **26**, 5198.

6. G. Sheldrick, *Acta Cryst., Sec. C*, 2015, **71**, 3.

7. I. S. Park, H. Komiyama and T. Yasuda, *Chem. Sci.*, 2017, **8**, 953.

8. Gaussian 16 (Revision A.03) M. J. Frisch, G. W. Trucks, H. B. Schlegel, G. E. Scuseria, M. A. Robb, J. R. Cheeseman, G. Scalmani, V. Barone, G. A. Petersson, H. Nakatsuji, X. Li, M. Caricato, A. V. Marenich, J. Bloino, B. G. Janesko, R. Gomperts, B. Mennucci, H. P. Hratchian, J. V. Ortiz, A. F. Izmaylov, J. L. Sonnenberg, D. Williams-Young, F. Ding, F. Lipparini, F. Egidi, J. Goings, B. Peng, A. Petrone, T. Henderson, D. Ranasinghe, V. G. Zakrzewski, J. Gao, N. Rega, G. Zheng, W. Liang, M. Hada, M. Ehara, K. Toyota, R. Fukuda, J. Hasegawa, M. Ishida, T. Nakajima, Y. Honda, O. Kitao, H. Nakai, T. Vreven, K. Throssell, J. A. Montgomery, Jr., J. E. Peralta, F. Ogliaro, M. J. Bearpark, J. J. Heyd, E. N. Brothers, K. N. Kudin, V. N. Staroverov, T. A. Keith, R. Kobayashi, J. Normand, K. Raghavachari, A. P. Rendell, J. C. Burant, S. S. Iyengar, J. Tomasi, M. Cossi, J. M. Millam, M. Klene, C. Adamo, R. Cammi, J. W. Ochterski, R. L. Martin, K. Morokuma, O. Farkas, J. B. Foresman and D. J. Fox, Gaussian, Inc., Wallingford CT, 2016.

9. H. Sun, C. Zhong and J.-L. Brédas, *J. Chem. Theory Comput*., 2015, **11**, 3851.